

# Influence of Molecular Architecture on the Adsorption of Poly(ethylene oxide)–Poly(propylene oxide)–Poly(ethylene oxide) on PDMS Surfaces and Implications for Aqueous Lubrication

Seunghwan Lee, Rico Iten, Markus Müller, and Nicholas D. Spencer\*

Laboratory for Surface Science and Technology, Department of Materials, Swiss Federal Institute of Technology, ETH Hönggerberg, Wolfgang-Pauli-Strasse 10, CH-8093, Zürich, Switzerland

Received May 11, 2004; Revised Manuscript Received August 2, 2004

**ABSTRACT:** We have investigated the adsorption and lubrication properties of a series of poly(ethylene oxide)–poly(propylene oxide)–poly(ethylene oxide) (PEO–PPO–PEO) block copolymers (“Pluronic”) to examine the feasibility of using them as aqueous lubricant additives. The adsorption behavior of PEO–PPO–PEO onto poly(dimethylsiloxane) (PDMS) surfaces was studied by optical waveguide lightmode spectroscopy (OWLS). The amount of adsorbed PEO–PPO–PEO copolymer exhibited a systematic variation, mainly according to the formula weight of the PPO block, and was found to increase with increasing PPO block size. The lubricating properties of the copolymers were investigated by means of pin-on-disk tribometry, employing self-mated PDMS as a tribo-pair in an aqueous environment. The lubricating behavior of the PEO–PPO–PEO copolymers was observed to be closely associated with their adsorption properties onto the PDMS surface; effective lubrication under low-velocity conditions was observed for those PEO–PPO–PEO copolymers that exhibited a significant adsorption of the PPO block, yet a significant role of the PEO block was also observed. The lubrication capabilities of PEO–PPO–PEO copolymers in aqueous media were attributed to the reduction of the hydrophobic interaction between PDMS surfaces by coating the surface with the copolymer and facilitating the formation of an aqueous lubricating film at the sliding interface.

## 1. Introduction

Poly(ethylene oxide)–poly(propylene oxide)–poly(ethylene oxide) (PEO–PPO–PEO) constitutes a group of amphiphilic block copolymers, often known as “Pluronic” (BASF Co.), which has found a broad range of industrial applications such as in detergents, dispersion stabilization, emulsification, and pharmaceuticals.<sup>1,2</sup> Adsorption of PEO–PPO–PEO block copolymers at solid/liquid interfaces in aqueous environments has been extensively investigated by employing several experimental approaches, including ellipsometry,<sup>3–5</sup> surface plasmon resonance (SPR),<sup>6–8</sup> photocalorimetry spectroscopy (PCS),<sup>9,10</sup> zeta potential measurements,<sup>11</sup> and sum-frequency generation (SFG).<sup>12</sup> The adsorption of PEO–PPO–PEO copolymers has been found to be most effective on hydrophobic surfaces.<sup>1–3,5,7–9</sup> At the solid/liquid interface in an aqueous environment, PEO–PPO–PEO copolymers have been shown to display a behavior whereby the central hydrophobic PPO block is anchored onto the hydrophobic solid surface, while the hydrophilic PEO blocks extend away into the bulk solution.<sup>1–3,5,7–9</sup> To date, PEO–PPO–PEO copolymers have been observed to adsorb on most common hydrophobic model surfaces, such as polystyrene,<sup>6,7,9</sup> hydrophobized silicon or glass,<sup>3,5</sup> and hydrophobic alkanethiol-based self-assembled monolayers (SAMs).<sup>8</sup>

Recently, the authors have shown that surface-immobilized PEG brushes, attached via copolymerization with poly(L-lysine) (PLL), thus generating poly(L-lysine)-*graft*-poly(ethylene glycol) (PLL-*g*-PEG),<sup>13,14</sup> can behave as effective aqueous boundary lubricant additives for oxide-based tribological systems.<sup>15–18</sup> Although aqueous lubrication holds several advantages compared

with conventional oil-based lubrication, namely its environmental compatibility, high heat capacity, and low cost, the extremely low pressure-coefficient of viscosity of water generally rules out the formation of a lubricating film under boundary conditions.<sup>19,20</sup> In a conformal contact where low-modulus elastomeric (LME) materials are involved, however, the elastic deformation of the contacting surfaces is often significant enough to generate a fluid film separating them.<sup>20–27</sup> Several previous studies have shown that sliding contact between highly elastic materials, typically rubber, and rigid materials exhibited an extremely low coefficient of friction,  $\sim 0.01$ , when the tribo-pair was lubricated by water.<sup>23–25</sup> The remarkable water-based lubricating performance of natural articular joints has also been ascribed, in large part, to the compliance of cartilage rather than just to the composition of synovial fluid itself.<sup>28–30</sup> Advantages of employing an LME coating for bearing systems have been long recognized.<sup>22–27</sup> However, the failure of the fluid film in such systems often leads to an increase in adhesive friction in the presence of smooth elastomeric materials.<sup>27</sup> Thus, the control of the surface properties of LME materials may be of critical importance to ensure their effective aqueous lubrication. To date, while the influence of elasticity and roughness of LME materials on their lubrication has been widely investigated,<sup>23–27</sup> less attention has been paid to the modification of the surface properties of LME materials other than the use of some simple surfactants.

In this work, we have investigated the adsorption and lubrication properties of PEO–PPO–PEO copolymers to examine the feasibility of using the copolymer as an additive for aqueous lubrication of an elastic sliding contact. For both adsorption and lubrication studies, a hydrophobic elastomer, poly(dimethylsiloxane) (PDMS), was selected as a model surface. In contrast to other

\* Corresponding author: Tel: +41 1 632 58 50; Fax: +41 633 10 27; e-mail: nicholas.spencer@mat.ethz.ch.

**Table 1. PEO–PPO–PEO Copolymers Used in This Study**

group	notation	total weight [g/mol]	PPO weight [g/mol]	PEO weight [g/mol]	PEO [wt %]	composition
PPO-900MW series	L31	1100	990	110	10	EO <sub>1</sub> PO <sub>17</sub> EO <sub>1</sub>
	L35	1900	950	950	50	EO <sub>11</sub> PO <sub>16</sub> EO <sub>16</sub>
	F38	4700	940	3760	80	EO <sub>43</sub> PO <sub>16</sub> EO <sub>43</sub>
PPO-1800MW series	L61	2000	1800	200	10	EO <sub>2</sub> PO <sub>31</sub> EO <sub>2</sub>
	P65	3400	1700	1700	50	EO <sub>19</sub> PO <sub>29</sub> EO <sub>19</sub>
	F68	8400	1680	6720	80	EO <sub>76</sub> PO <sub>29</sub> EO <sub>76</sub>
PPO-3000MW series	L101	3800	3420	380	10	EO <sub>4</sub> PO <sub>59</sub> EO <sub>4</sub>
	P105	6500	3250	3250	50	EO <sub>37</sub> PO <sub>56</sub> EO <sub>37</sub>
	F108	14600	2920	11680	80	EO <sub>133</sub> PO <sub>50</sub> EO <sub>133</sub>

previously studied hydrophobic surfaces mentioned above, PDMS possesses a distinctively lower modulus of elasticity (typically equal to or lower than 2 MPa) and thus can readily provide a conformal, low-pressure contact. Furthermore, PDMS can be easily fabricated into (hemi)spherical and plane shapes with a smooth surface finish. By selecting a series of PEO–PPO–PEO copolymers possessing systematically different structures, more specifically, PPO block molecular weight and PEO block molecular weight ratio, we have attempted to understand the influence of architectural features of the copolymer on its adsorption and lubrication properties.

## 2. Materials and Methods

**2.1. PEO–PPO–PEO and PEG.** The poly(ethylene oxide)–poly(propylene oxide)–poly(ethylene oxide) (PEO–PPO–PEO) copolymers were commercially available, standard materials and were kindly supplied by BASF (Mt. Olive, NJ). In this work, we have employed nine different types of PEO–PPO–PEO copolymers possessing systematically different PPO and PEO block molecular weights (Table 1). For the notation of PEO–PPO–PEO copolymers, the nomenclature system given by the manufacturer is used; the letter represents the physical form of the copolymer, “L” for liquids, “P” for pastes, and “F” for flakes; the first (or first two) number(s) represent(s) the molecular weight of the PPO block (when multiplied by 300, this yields the approximate PPO block molecular weight, g/mol), and the last number represents the molecular weight ratio of the PEO block (when multiplied by 10, this yields the approximate percentage of the PEO block in the total molecular weight). As mentioned in many previous studies,<sup>1</sup> the molecular weight and PEO ratio given by the manufacturer, which are quoted in Table 1, are only approximate and vary, often significantly, from batch to batch. The polydispersity ( $M_w/M_n$ ) of the PEO–PPO–PEO copolymers was not measured, but values have been reported in the literature to lie between 1.1 and 1.2.<sup>4,10</sup> It is noted that the selected PEO–PPO–PEO copolymers in this work can be classified into three groups according to the central PPO block molecular weight (MW): (1) PPO-900MW series, L31, L35, and F38; (2) PPO-1800MW series, L61, P65, and F68; (3) PPO-3000MW series, L101, P105, and F108. The selected PEO–PPO–PEO copolymers can also be classified according to the PEO molecular weight ratio: (a) PEO-10% series, L31, L61, and P101; (b) PEO-50% series, L35, P65, and P105; (c) PEO-80% series, F38, F68, and F108. For comparison with the PEO–PPO–PEO copolymer, poly(ethylene glycol) (PEG) homopolymers with molecular weights of 2000 and 6000 were also purchased (Fluka, Switzerland).

**2.2. Aqueous Polymer Solution and Viscosity.** All polymers were dissolved in aqueous buffer solution (pH ~7, buffered by 10 mM KH<sub>2</sub>PO<sub>4</sub> and pH adjusted by 6 M KOH). For tribological measurements, the copolymer concentration was varied from 0.02 to 5 mg/mL. For adsorption measurements, the copolymer concentration was 2 mg/mL. The viscosity of the PEO–PPO–PEO aqueous solutions, as well as water and buffer solution, was measured using a UDS 2000 rheometer in Couette geometry (Physica Messtechnik, Ostfildern,

**Table 2. Measured Viscosity of the PEO–PPO–PEO Copolymers (2 mg/mL) in Buffer Solution (pH 7)**

group	notation	viscosity ( $\times 10^{-3}$ Pa s)
PPO-900MW series	water	1.0
	buffer	1.0
	L31	1.1
	L35	1.1
PPO-1800MW series	F38	1.1
	L61	1.1
	P65	1.0
	F68	1.1
PPO-3000MW series	L101	1.0
	P105	1.1
	F108	1.1

Germany). The viscosity was obtained from the slope of the linear part (from  $10^2$  to  $10^3$  s<sup>-1</sup>) of the shear strain vs shear rate plot. The results are summarized in Table 2. All chemicals were reagent grade and purchased from Sigma-Aldrich (St. Louis, MO).

**2.3. Optical Waveguide Lightmode Spectroscopy (OWLS).** Optical waveguide lightmode spectroscopy (OWLS)<sup>31–34</sup> was employed to investigate the adsorption behavior of the PEO–PPO–PEO copolymers onto a PDMS surface. OWLS is based upon grating-assisted in-coupling of a He–Ne laser into a planar waveguide and allows a direct online monitoring of the “dry” mass of macromolecule adsorption, in that water that is hydrodynamically coupled into adsorbates is not taken into account in mass detection. This method is highly sensitive out to a distance of ~200 nm from the surface of a waveguide (sensitivity limit, ~1 ng/cm<sup>2</sup>). Furthermore, a measurement time resolution of 3 s allows the in-situ, real-time study of adsorption kinetics. The waveguide chips used for OWLS measurements were purchased from MicroVacuum Ltd. (Budapest, Hungary) and consist of a 1 mm thick AF 45 glass substrate with a 200 nm thick Si<sub>0.75</sub>Ti<sub>0.25</sub>O<sub>2</sub> waveguiding layer at the surface. The waveguides were further coated with ultrathin PDMS films using a spin-coater. The base and curing agent of a commercial silicone elastomer, SYLGARD 184 elastomer kit (Dow Corning, Midland, MI), were dissolved in hexane at a ratio of 10:3 (total concentration 0.5 wt %) and spin-coated onto the waveguide. After spin-coating at 2000 rpm for 40 s, the waveguides were removed from the spinner disk and cured in an oven at ~70 °C overnight. The thickness of the thin PDMS films generated by this method was ca. 30 nm, and the static water contact angle was  $100 \pm 2^\circ$ .

All OWLS experiments were carried out in a BIOS-I instrument (ASI AG, Zürich, Switzerland) using a Kalrez (Dupont, Wilmington, DE) flow-through cell ( $8 \times 2 \times 1$  mm).<sup>30</sup> The PDMS-coated waveguide was first exposed to buffer solution until a stable baseline was obtained. Then, PEO–PPO–PEO solution was injected into the flow cell. The change in refractive index in the vicinity of the surface upon injection of the polymer solution reflects the adsorption of the polymers. However, it is also influenced by the refractive index of the bulk polymer solution itself, and this effect is of significance, especially for turbid solutions. The adsorbed mass was thus measured only after the flow cell was rinsed with buffer solution. For this reason, the adsorbed mass in this work does not include weakly surface-bound copolymers, which may play

a significant role in lubricating properties, as will be addressed below. Adsorbed mass density data were calculated according to de Feijter's formula from the adsorbed layer thickness and refractive index values from the mode equations.<sup>35</sup> A refractive index increment ( $dn/dc$ ) value of  $0.151 \text{ cm}^3/\text{g}$  was used for the calculation of PEO-PPO-PEO adsorption.<sup>4,36</sup>

**2.4. Pin-on-Disk Tribometry.** The lubrication properties of PEO-PPO-PEO copolymers have been characterized by means of a pin-on-disk tribometer (CSM, Neuchâtel, Switzerland). In this approach, a loaded pin (controlled by a dead weight) is brought into contact with a flat disk, both of which were fully immersed in the lubricant. In this work, the lubricants consist of the polymer-containing aqueous solutions that are mentioned above. After forming a lubricated contact, the disk is rotated at a controlled speed by a motor, thus generating sliding interfacial friction forces. The friction forces were measured by a strain gauge. More detailed information on the pin-on-disk tribometer and operational principles are to be found in previous publications.<sup>16,17,37</sup>

The friction measurements were started 15 min after the aqueous lubricant solution was transferred into the cell in which the pin/disk contact was to occur, to allow adsorption of the PEO-PPO-PEO copolymers onto the PDMS surface. The polymers generally remained in the bulk lubricant solution during friction measurements unless otherwise mentioned. As control experiments, friction measurements were also performed in which the polymer-containing aqueous solutions were replaced with buffer solution.

To investigate the influence of concentration and copolymer architecture on the lubrication properties, a  $\mu$  ( $\mu = F/L$ , where  $F$  is friction force and  $L$  is load) vs speed plot was obtained for each case under a fixed load (1 N). The speed was varied from 0.001 to 0.1 m/s. For all cases, i.e., for all architectures of PEO-PPO-PEO, concentrations, and sliding speeds, the aqueous-solution-lubricated sliding of the PDMS/PDMS tribo-pair rapidly reached a steady kinetic friction force,  $F_k$ , after only a few rotations. The number of rotations was 20 for each measurement. The average friction force from the latter half of these (11th to 20th) was obtained to avoid "running-in" effects. For control experiments, the sliding speed was fixed at 0.005 m/s, and the load was varied from 0.5 to 5 N, and thus a friction vs load plot was obtained.

**2.5. Tribo-pair.** Poly(dimethylsiloxane) (PDMS) has been employed for both pin and disk materials and was prepared from a commercial silicone elastomer kit (SYLGARD 184 silicone elastomer, base and curing agent, Dow Corning, Midland, MI). To prepare the hemispherical PDMS pin and the disk, corresponding masters were prepared; a commercial polystyrene cell-culture plate with round-shaped wells (96 MicroWell Plates, NUNC/NON Delta Surface, Roskilde, Denmark) was used as a pin master (radius 3 mm), and a home-machined aluminum plate with flat wells (diameter 30 mm and depth 5 mm) was used as a disk master. The PDMS pin and disk were prepared according to a conventional recipe.<sup>38</sup> Briefly, the base and curing agent of the SYLGARD 184 elastomer kit were mixed at 10:1 ratio (by weight). The foams generated during mixing were removed by house vacuum. The mixture was transferred into the masters and incubated in an oven ( $\sim 70^\circ\text{C}$ ) overnight. The static water contact angle and the elasticity modulus of the PDMS generated in this method were  $110 \pm 2^\circ$  and  $\sim 2 \text{ MPa}$ , respectively. For the disk, the side exposed to air during curing was used for the friction measurements. The roughness of the PDMS disk was characterized as  $\sim 0.5 \text{ nm}/10 \mu\text{m}^2$  by atomic force microscopy (Dimension 3000, Digital Instruments, Santa Barbara, CA). The roughness of the pin was estimated as  $\sim 2 \text{ nm}/\mu\text{m}^2$  by measuring the morphology of the polystyrene master by AFM.

Finally, it is noted that one PDMS pin and disk pair was used for only one measurement and was replaced by another pair for the next measurements to avoid cross-contamination.

### 3. Results

**3.1. Adsorption Properties.** The adsorption behavior of PEO-PPO-PEO copolymers onto the PDMS

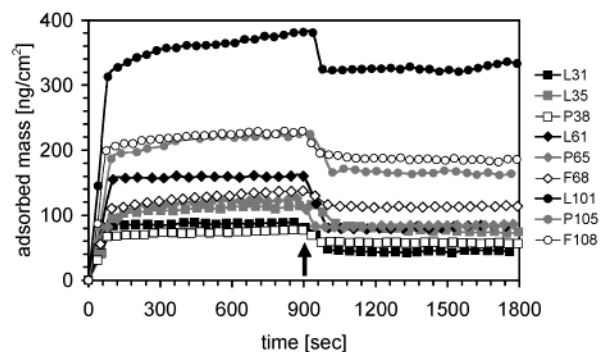


**Figure 1.** Adsorbed mass vs time plots of PEO-PPO-PEO copolymers on a PDMS surface by optical waveguide lightmode spectroscopy (OWLS). The concentration was  $2.0 \text{ mg/mL}$  and the pH was 7. The arrow ( $\sim 900 \text{ s}$ ) indicates the buffer rinsing.

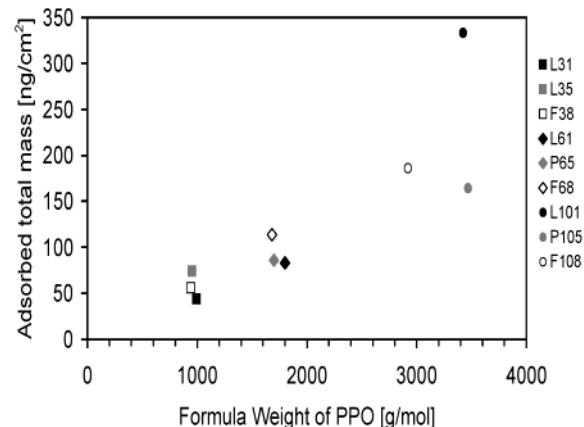


**Figure 2.** Mass of the adsorbed PEO-PPO-PEO copolymers on a PDMS surface plotted as a function of formula weight of the PPO blocks. The concentration was  $2.0 \text{ mg/mL}$  and the pH was 7.

surface was characterized by means of OWLS. The concentration of the copolymer solution was  $2 \text{ mg/mL}$  for all cases. As will be detailed below, the selection of this concentration was motivated by the copolymer's lubrication properties (see the section 3.2). The mass uptake vs time plots for all PEO-PPO-PEO copolymers are presented in Figure 1. Upon exposure of a PDMS-coated waveguide to a PPO-PEO-PPO copolymer solution, at  $t = 0$ , the mass uptake rapidly reached near saturation (within  $\sim 300 \text{ s}$ ) for all cases. By rinsing the flow cell with buffer solution, at  $t = \sim 900 \text{ s}$ , some portion of the initially adsorbed polymers desorbed. The final mass of adsorbed polymer was obtained by monitoring the mass at  $t = \sim 1800 \text{ s}$ .

To examine the relationship between the adsorption properties with the structural features of PEO-PPO-PEO copolymer, the final masses (at  $t = \sim 1800 \text{ s}$  in Figure 1) of adsorbed PEO-PPO-PEO copolymers are plotted against the formula weights of PPO blocks in Figure 2. The mass of adsorbed PEO-PPO-PEO copolymer increased with increasing formula weight of PPO block roughly in a linear fashion.

Assuming that the PPO block and PEO block contribute equally to the OWLS signal change (refractive index) due to mass uptake of the PEO-PPO-PEO copolymer, the adsorbed PEO and PPO block mass can be estimated according to the molecular weight ratio of each block as given in Table 1. First, the estimated mass of adsorbed PPO block in this way is plotted against the formula weight of PPO block in Figure 3a. For a



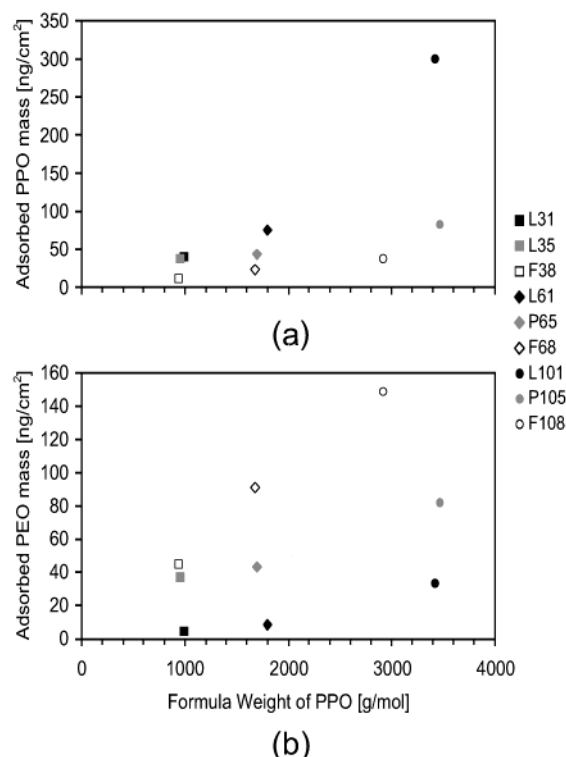


**Figure 3.** (a) PPO block mass and (b) PEO block mass of the adsorbed PEO-PPO-PEO copolymers on PDMS surfaces plotted vs formula weight of the PPO blocks. The concentration was 2.0 mg/mL and the pH was 7.

given PPO series, the adsorbed PPO mass appears to decrease with increasing PEO ratio, and this trend is clearer with increasing formula weight of PPO. For a given series of fixed PEO ratio, however, the adsorbed PPO mass increased with increasing formula weight of PPO. Second, the estimated mass of adsorbed PEO is plotted against the formula weight of PPO block in Figure 3b. For each PPO series, the adsorbed PEO mass increased with increasing PEO ratio. In addition, for each series of fixed PEO ratio, the adsorbed PEO mass also increased with increasing PPO formula weight. The results of adsorbed total mass and the fractions of PEO and PPO block are listed in Table 3.

Finally, the adsorption of PEG homopolymers, both 2000 and 6000 MW onto a PDMS surface, was observed to be negligible ( $<3$  ng/cm<sup>2</sup>, data not shown).

**3.2. Lubrication Properties.** The lubrication properties of PEO-PPO-PEO copolymers in aqueous solution have been characterized by means of pin-on-disk tribometry. First, the concentration dependence of

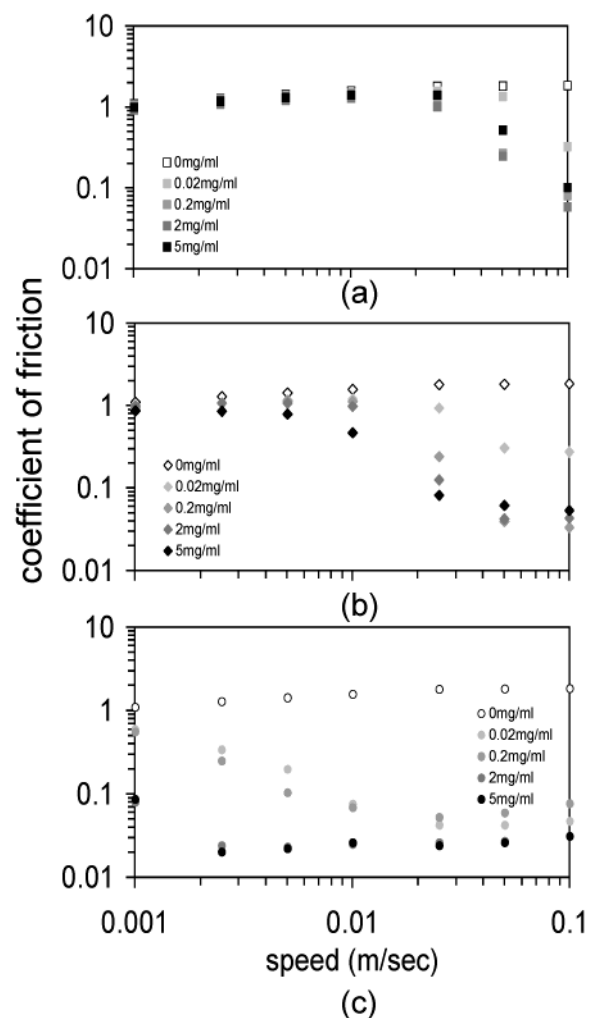


**Figure 4.** Coefficient of friction vs speed plots (aqueous lubrication of PDMS vs PDMS) for (a) L35, (b) P65, and (c) P105 as a function of PEO-PPO-PEO copolymer concentration (0.02, 0.2, 2.0, and 5.0 mg/mL). The error bar in the coefficient of friction, typically 0.02, has not been shown, for clarity.

lubrication properties of some selected PEO-PPO-PEO copolymers, including PEO-50% series, L35, P65, P105, and PPO-1800MW series, L61, P65, F68, was investigated. The selected concentrations were 0.02, 0.2, 2, and 5 mg/mL. At each concentration, the  $\mu$  vs speed plot was obtained. The results for the PEO-50% series are presented in Figure 4. For all three PEO-PPO-PEO copolymers, the  $\mu$  values were observed to decrease with increasing concentration. However, the degree of reduc-

**Table 3.** Mass of Adsorbed PEO-PPO-PEO Copolymer, Fractions of PPO and PEO Blocks, and Relative Formula Weights of PPO and PEO Blocks<sup>a</sup>

group	notation	A	B	C	D	E	F	G
PPO-900MW series	L31	43.9	39.5	1.00	1.00	4.4	1.00	1.00
	L35	74.2	37.1	0.94	0.96	37.1	8.44	8.64
	F38	55.9	11.2	0.78	0.95	44.7	10.19	34.18
PPO-1800MW series	L61	83.1	74.8	1.00	1.00	8.3	1.00	1.00
	P65	86.0	43.0	0.57	0.94	43.0	5.17	8.50
	F68	113.7	22.7	0.30	0.93	91.0	10.95	33.60
PPO-3000MW series	L101	333.3	300.0	1.00	1.00	33.3	1.00	1.00
	P105	164.0	82.0	0.27	1.01	82.0	2.46	3.91
	F108	185.8	37.2	0.12	0.85	148.6	4.46	30.74

<sup>a</sup>A = the mass of adsorbed PEO-PPO-PEO copolymers [ng/cm<sup>2</sup>], B = the mass of adsorbed PPO block [ng/cm<sup>2</sup>], C = the relative mass of the adsorbed PPO within each PPO series, D = the relative formula weight of the PPO block within each PPO series, E = the mass of tethered PEO block [ng/cm<sup>2</sup>], F = the relative mass of the adsorbed PEO block within each PPO series, and G = the relative formula weight of the PEO block within each PPO series.

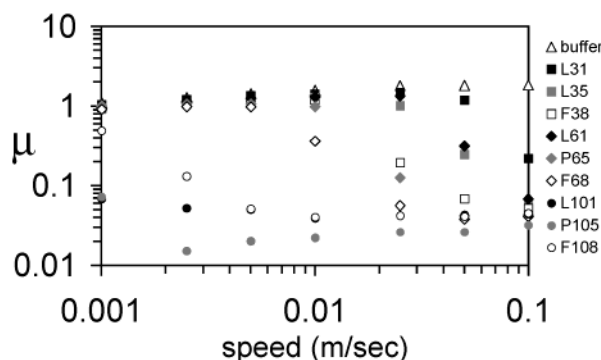


**Figure 5.** Coefficient of friction vs speed plots (aqueous lubrication of PDMS vs PDMS) for PEO-PPO-PEO copolymers at a concentration of 2.0 mg/mL. The error bar in the coefficient of friction, typically 0.02, has not been shown, for clarity.

tion in  $\mu$  due to copolymer concentration change is strongly influenced by the structure of the PEO-PPO-PEO copolymer. For L35 (Figure 4a), the reduction of  $\mu$  is not significant and observed only at very high speeds ( $\geq 0.05$  m/s). With increasing PPO molecular weight, i.e., on the order of L35 (Figure 4a), P65 (Figure 4b), and P105 (Figure 4c), the reduction of  $\mu$  starts at lower speeds, and the magnitude of reduction in  $\mu$  values is also greater at any given speed. The concentration-dependent lubrication behaviors of L61 and F68 in the PPO-1800MW series were indistinguishable from those of L35 and P65, respectively (data not shown).

From Figure 4, it is apparent that the reduction of  $\mu$  is almost saturated at 2 mg/mL for all cases. For this reason, the lubrication properties of all nine PEO-PPO-PEO copolymers have been characterized at 2 mg/mL. The results are shown in Figure 5. The PEO-PPO-PEO copolymers belonging to either the PPO-900MW series or the PPO-1800MW series did not show a significant lubricating effect except at high speeds ( $\geq 0.05$  m/s), although some of them, for instance F38, P65, and F68, showed a lubricating effect from relatively lower speeds ( $\geq 0.01$  m/s). In contrast, all three PEO-PPO-PEO copolymers belonging to the PPO-3000MW series showed noticeable reduction in  $\mu$  starting at very low speeds ( $\geq 0.001$  m/s). This observation suggests that the PPO molecular weight primarily determines the lubrication properties of PEO-PPO-PEO copolymers in an aqueous environment. Among the PPO-3000MW series, the lubricating effects of P101 and P105 at low speeds are clearly superior to those of F108.

To investigate the lubrication mechanism in more detail, two control experiments were performed by employing a "good" lubricant additive, e.g., P105. First, to examine the influence of the unbound copolymers in bulk lubricant solution, the copolymer-containing solution was replaced by buffer solution following adsorption, thus leaving the surface-bound PEO-PPO-PEO copolymers under polymer-free buffer. The  $\mu$  vs speed plot obtained in this approach is presented in Figure 6 (load 1 N). While the coefficients of friction at high speeds remained low and indistinguishable from those observed when the polymers are also present in the bulk solution, the coefficients of friction at low speeds were observed to increase with decreasing speed in the absence of polymer in solution. Second, the load-dependent friction forces were measured at a given speed (0.005 m/s) with and without P105 in buffer solution. The results are compared in Figure 7. For both cases,

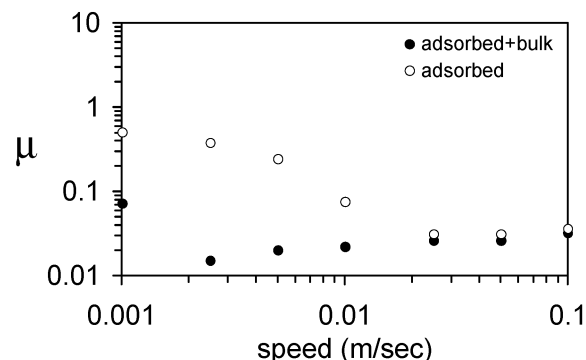


**Figure 6.** Coefficient of friction vs speed plots (aqueous lubrication of PDMS vs PDMS) for P105 before (●, adsorbed + bulk) and after (○, adsorbed) the copolymer-containing solution was replaced by buffer solution. The error bar in the coefficient of friction, typically 0.02, has not been shown, for clarity.

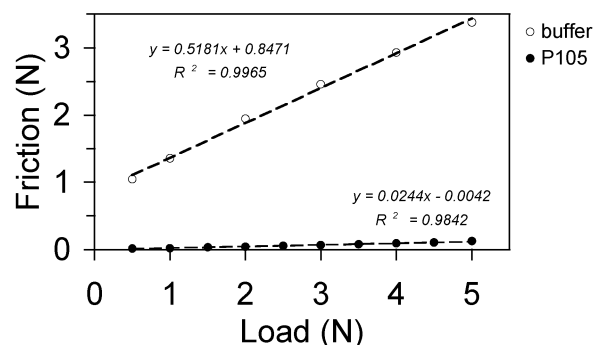


**Figure 7.** Friction vs load plot for the self-mated sliding of PDMS lubricated by buffer alone (○) and P105-containing buffer solution (●). The sliding speed was 0.005 m/s.

the friction forces increased in a linear fashion with increasing load ( $R^2 = 0.99$  for buffer only and 0.98 for P105-containing buffer solution), yet a significant reduction in friction force is observed upon the addition of P105 to the buffer solution (the slope of friction vs load plot  $dF/dL = 0.518$  for buffer only and 0.024 for P105). It is also noted that the  $y$ -intercept, a friction force extrapolated to zero applied load, reduced from 0.847 N to nearly zero ( $-0.0042$  N) upon addition of P105 into buffer solution.

Finally, the  $\mu$  vs speed plot was obtained by employing homopolymeric PEG as an aqueous lubricant additive at 2 mg/mL concentration. For both 2000 and 6000 MW, the lubrication effect was almost completely negligible (data not shown).

## 4. Discussion

**4.1. Adsorption Properties: Influence of Structural Features of PEO-PPO-PEO Copolymers.** In previous studies, it has been well documented that PEO-PPO-PEO copolymer adsorbs onto hydrophobic surfaces in an aqueous environment through the hydrophobic interaction of PPO block with the surfaces, and the PEO blocks stretch away from the solid/liquid interface.<sup>1-3,5,7-9</sup> This type of conformation appears to occur on the PDMS surface as well, since all PEO-PPO-PEO copolymers exhibit a finite amount of adsorption (Table 3), while the adsorption of homopolymeric PEG is negligible. As mentioned above, OWLS is sensitive to adsorbed "dry" mass change on a waveguide, and the vertical detection limit reaches out to  $\sim 200$  nm.<sup>32-34</sup> Since the length of the PEO chain for the

longest PEO case (F108) is 52.8 nm in its fully extended conformation,<sup>11</sup> all of the employed PEO-PPO-PEO copolymers are within the detection range of OWLS. Furthermore, the structural difference between PPO and PEO block is one methyl group per monomer. Thus, the total mass of adsorbed PEO-PPO-PEO copolymer can be decomposed into that of its PPO block and PEO block according to their molecular weight ratio (Table 3).

The estimated mass of adsorbed PPO and PEO blocks in this way provides more insights into the adsorption behavior of PEO-PPO-PEO copolymer onto the PDMS surface in aqueous media. As shown in Figure 3a, the amount of adsorbed PPO block exhibits an increasing trend with increasing PPO formula weight. For a fixed PPO block size, however, the adsorbed PPO mass shows a decreasing trend with increasing PEO % ratio, and this trend is clearer at higher PPO molecular weight. For instance, when the mass of adsorbed PPO of the PPO-900MW series is normalized by that of L31, the relative mass of the PPO block is 1.0:0.94:0.28 for L31:P35:P38, although the formula weight ratio is nearly constant (1.00:0.96:0.95). For the PPO-1800MW series, the relative mass of the adsorbed PPO is 1.00:0.57:0.30 for L61:P65:F68 (normalized by the PPO mass of L61), while the relative formula weight is 1.00:0.94:0.93. Finally, for the PPO-3000MW series, the relative mass of the adsorbed PPO is 1.00:0.27:0.12 (normalized by the PPO mass of L101), while the relative formula weight is 1.00:1.01:0.85. Given that adsorption of PEO-PPO-PEO copolymers onto hydrophobic surfaces occurs exclusively through the interaction of the PPO block with the surface, the reduced adsorption of the PPO block with increasing PEO % ratio is translated into a reduced total amount of tethered PEO block (see Table 3 for detailed comparison). The reduced adsorption of PEO-PPO-PEO copolymers with increasing PEO molecular weight is, in fact, a general behavior on hydrophobic surfaces, although it has not been highlighted in previous studies.<sup>1-3,5,7-9</sup> This behavior is primarily attributed to the higher solubility of PEO-PPO-PEO copolymers possessing a high PEO ratio. With increasing PEO molecular weight, the PEO-PPO-PEO copolymers can remain stabilized in bulk solution even without the need for micellization,<sup>6</sup> and thus the driving force to adsorb onto the surface is reduced. In addition, initial adsorption of PEO-PPO-PEO copolymers may prevent further adsorption of incoming copolymers more effectively when the molecular weight of the PEO block becomes higher, due to enhanced PEO-PEO repulsion.

It is emphasized that the decomposition of the adsorbed mass of PEO-PPO-PEO copolymers into the corresponding masses of PPO and PEO blocks is only possible because OWLS is sensitive to the "dry" mass of adsorbed moieties on surfaces without taking into account the hydrodynamically coupled water. This approach offers a more in-depth understanding of the respective behavior of the PEO and PPO blocks in the adsorption of PEO-PPO-PEO copolymers, and its usefulness is highlighted when the PEO-PPO-PEO-coated surface is utilized for further applications, as shown in the following section.

**4.2. Lubrication Properties: Influence of Adsorption Behavior of PEO-PPO-PEO Copolymers.** The frictional properties of self-mated PDMS in an aqueous environment have been observed to be significantly influenced by the addition of PEO-PPO-

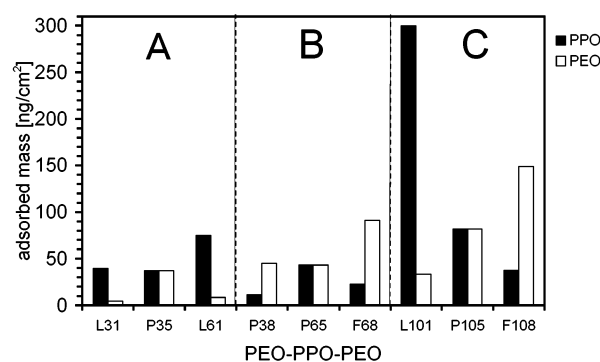


**Figure 8.** PPO block and PEO block masses of adsorbed PEO-PPO-PEO copolymers onto PDMS surfaces classified according to their lubrication behavior.

PEO copolymers into the solution. In addition, the degree of lubrication has also been strongly correlated with the structural features of the PEO-PPO-PEO copolymers. As shown in Figure 5, the lubrication properties of PEO-PPO-PEO copolymers are primarily determined by the molecular weight of the central PPO block; the lubrication effect is enhanced roughly in the order of PPO-900MW series < PPO-1800MW series < PPO-3000MW series. This is attributed to the primary role of PPO block in the adsorption properties of the PEO-PPO-PEO copolymer onto a PDMS surface. As an extreme case, homopolymeric PEG polymer solution showed virtually no improvement in the lubrication properties compared with buffer solution.

To examine the role of PPO and PEO block in the aqueous lubrication properties of PEO-PPO-PEO copolymers in more detail, the estimated mass of adsorbed PPO and PEO blocks (Table 2 and Figure 3) is directly compared with the lubrication properties in Figure 8. It should be noted that the amount of adsorbed copolymers for the tribological measurements could be slightly different from that for the OWLS measurements due to possible differences in the degree of cross-linking of the PDMS, related to thickness effects. However, the overall trend is believed to remain unaltered. Since the lubrication properties cannot be readily expressed by a single number, copolymers exhibiting similar lubrication properties are grouped together: group A, showing negligible lubricating effect except at very high speed ( $\geq 0.05$  m/s), includes L31, P35, and L61; group B, showing lubricating effect from intermediate speeds ( $\geq 0.01$  m/s), includes P38, P65, and F68; and finally group C, showing a lubricating effect from very low speeds ( $\geq 0.001$  m/s), includes L101, P105, and F108. It is noted that this classification is quite similar to that according to the PPO molecular weight, yet not identical (exception e.g. L61 and P38). A comparison of the adsorbed PPO and PEO molecular weight with the lubricating properties in Figure 8 provides some insights into the role of each block in aqueous lubrication properties of the copolymers. First, the relative mass of adsorbed PPO of the PEO-50% series is 1.00:1.16:2.21 for P35:P65:P105 (normalized by the adsorbed PPO mass of P35), while the lubricating behavior of each copolymer showed the characteristic of group A (P35), B (P65), and C (P105), respectively (Figure 8). The enhanced lubricating effect in the order of P35 < P65 < P105 can be, of course, attributed to increased mass of adsorbed PPO and consequently PEO blocks, too, yet the difference, especially between P35 and P65 (37.1 vs 43.0 ng/cm<sup>2</sup>), is not high enough to be convincing. This



observation indicates that it is not only the adsorbed PPO mass itself, but the PPO block molecular weight, i.e., number of anchoring units ( $\text{CH}_3-$  groups), also needs to be taken into account to explain the observed lubrication effect. The relative PPO length or number of anchoring groups of the PEO-50% series is 1.00:1.81:3.50 (Table 2, normalized by the PPO formula mass of P35). It is clear that stable anchoring of the polymer becomes critical when the polymer-coated surface is subjected to sliding contact.

Second, the PPO-3000MW series, L101, P105, and F108, shows an opposite trend in the adsorbed mass of PPO and PEO block (1.00:0.27:0.12 for PPO and 1.00:2.46:4.46 for PEO when normalized by adsorbed PPO and PEO of L101), and the lubricating effect is in the order of  $F108 < L101 \leq P105$  (the lowest friction), although all of them belong to group C (Figure 8). This observation further supports our contention that the PPO block mainly determines the lubricating properties of PEO-PPO-PEO copolymers. However, comparison of F108 with many other PEO-PPO-PEO copolymers shows that the PEO block also contributes to lubrication to a certain degree. For instance, L31, L35, L61 (group A), and P65 (group B) exhibited a higher amount of the PPO block than F108 (group C), yet an inferior lubrication effect to F108. This difference may be partly due to the longer PPO block length of F108 as mentioned above but is strongly associated with the higher amount of PEO block in F108. The PEO block is believed to enhance the lubrication by reducing the hydrophobic interaction between PDMS surfaces in aqueous media and thus facilitating the entrainment of lubricant into the sliding interface.

Third, the comparison of P105 and F68/L61 further supports the significant roles of both the PPO and PEO blocks in the aqueous lubrication properties of PEO-PPO-PEO copolymers. The mass of the tethered PEO block of F68 ( $91 \text{ ng/cm}^2$ ) is even slightly higher than that of P105 ( $82 \text{ ng/cm}^2$ ), yet a much more effective lubrication is observed from P105 (group C) than F68 (group B). The difference can be ascribed to the smaller amount of adsorbed PPO for F68 ( $22.7 \text{ ng/cm}^2$ ) than that for P105 ( $82 \text{ ng/cm}^2$ ) as well as the shorter PPO block length of the F68, as discussed above. The mass of adsorbed PPO for L61 ( $74.8 \text{ ng/cm}^2$ ) is also comparable to that of P105 ( $82 \text{ ng/cm}^2$ ), while that of the PEO block for L61 is negligible ( $8.3 \text{ ng/cm}^2$ ) and smaller than that of P105 by an order of magnitude ( $82 \text{ ng/cm}^2$ ). The lubricating properties of each copolymer showed the characteristics of group A for L61 and group C for P105 (Figure 8). Although the shorter PPO length of L61 may be partially responsible, the significantly smaller amount of adsorbed PEO block of L61 is well correlated with its inferior lubricating properties when compared to P105.

**4.3. Lubrication Properties: Influence of Unbound PEO-PPO-PEO Copolymers.** Results from a control experiment (Figure 6) show that removal of unbound PEO-PPO-PEO copolymers from the bulk solution results in a degradation of lubrication in the low-speed regime. Two mechanisms can be proposed for this behavior. First, shear motion of two PDMS surfaces can generate a transient detachment of adsorbed polymers and a subsequent readsorption of the unbound or detached polymers when they are available in the medium surrounding the sliding interface. In contrast, the removal of copolymers from the solution would

reduce the probability of readsorption due to reduced concentration of available polymers. It is noted, however, that the degradation of the lubricating effect by replacing the copolymer with buffer is exclusively observed in the low-speed regime (Figure 6). Since pin-on-disk tribometry allows repeated sliding over a fixed track, if the tribo-induced desorption and readsorption is the dominant mechanism, readsorption should be more probable at lower speeds for kinetic reasons.

Second, the unbound copolymers could contribute to lubrication by being entrained into the sliding interface. However, as shown in Table 2, the bulk viscosity of the PEO-PPO-PEO copolymer was not distinguishable from that of water or buffer solution, regardless of structural features of the copolymer. Thus, as the thickness of the lubricating film becomes high enough to entrain bulk solution, the presence of unbound copolymer in bulk solution would hardly make a difference, which is probably the case for the high-speed regime. However, when the thickness of lubricating film becomes small at lower speeds, the presence of unbound copolymers could contribute to the formation of more effective boundary lubricating films due to an increased effective viscosity. In previous studies,<sup>39,40</sup> Smeeth and co-workers have shown that the addition of polyisoprene and other polymers into base oil resulted in an abnormal increase of the lubricant film thickness at low speed under rolling contact. In that work, the viscosity of the lubricant when the film thickness is smaller than 20 nm was estimated to be 10–20 times higher than that of bulk lubricant. In other work by Roberts and Tabor,<sup>22</sup> the viscosity of thin ( $<20 \text{ nm}$ ) water films during rubber/glass sliding contact was observed to be ca. 2.5 times higher than that of bulk water when sodium dodecyl sulfate (SDS) was added (10 mmol) into water. The current situation is slightly different from these in that the difference is seen for unbound copolymers in the bulk solution, while adsorbed polymers are equally present for both cases. However, since the degradation of the lubricating effect is observed only at slow speeds without unbound copolymer in bulk solution (Figure 6), it is very plausible that a similar mechanism is also active in this case.

**4.4. Lubrication Properties: Influence of Hydrophobic Interactions in Self-Mated Sliding of PDMS.** Another control experiment in Figure 7 reveals that the lubrication mechanism by PEO-PPO-PEO copolymers is partly due to the removal of strong adhesion between the two PDMS surfaces. The hydrophobic interaction between PDMS surfaces has been extensively studied<sup>38,41–43</sup> and the work of adhesion determined to be  $42.2\text{--}50.7 \text{ mJ m}^{-2}$  in ambient<sup>38,41–43</sup> and  $75 \text{ mJ m}^{-2}$  in water.<sup>38</sup> Thus, the finite friction forces at zero load ( $\sim 0.85 \text{ N}$  under a load of 1 N) when the friction vs load plots in Figure 7 are extrapolated can be attributed to adhesive friction of self-mated PDMS surface in aqueous solution. As mentioned above, the hydrophilic characteristics of the tethered PEO block can effectively reduce the hydrophobic interaction between PDMS surfaces; thus, the finite friction at zero load vanished upon addition of P105 (Figure 7).

## 5. Conclusions

In this work, we have demonstrated that PEO-PPO-PEO copolymers can be used as effective additives for the aqueous lubrication of an elastomer, PDMS, by investigating the adsorption and lubrication properties

in parallel. The prime purpose of this work was to understand the role of structural features, more specifically the molecular weight of the PPO block and the molecular weight ratio of PEO block, in adsorption and lubrication. The adsorption properties of PEO-PPO-PEO copolymers onto PDMS surfaces have been studied by means of OWLS in an aqueous environment. The amount of adsorbed PEO-PPO-PEO copolymer systematically increased with increasing PPO block formula weight. The "dry" mass of adsorbed PEO-PPO-PEO copolymers, determined by OWLS, was further decomposed into that of the PPO and PEO blocks. Holding the PPO block size constant, increasing the PEO molecular weight resulted in an increase in the adsorbed amount of the PEO block, yet a decrease in the adsorbed amount of PPO block. The lubricating properties (pin-on-disk tribometry) of PEO-PPO-PEO copolymers have been observed to be mainly determined by the formula weight and adsorbed amount of PPO block; the higher the PPO molecular weight, the better the lubrication properties. This observation suggests that stable anchoring of PEO-PPO-PEO copolymers onto the PDMS surface is the most important factor for effective lubrication. However, comparative studies of adsorption and lubrication properties of a variety of PEO-PPO-PEO copolymers revealed that a greater amount of adsorbed PEO block also contributes to better lubrication. The effective aqueous lubrication of PDMS surface by means of adsorbed PEO-PPO-PEO copolymers is attributed partly to the reduction of strong hydrophobic interactions between PDMS surfaces in aqueous media and thus facilitates the formation of lubricating films.

**Acknowledgment.** The authors gratefully acknowledge BASF for the supply of the PEO-PPO-PEO copolymers, Dr. Kirill Feldman for his help in spin-coating of PDMS film onto OWLS waveguides, Dr. Janos Vörös for the advice in OWLS measurements and useful discussion in analyzing OWLS data, and Dr. Thomas Schweizer for his help in viscosity measurements. This work has been supported by the U.S. Air Force Office of Scientific Research under Contract F49620-02-1-0346 and the TopNano21 Program of the Council of the Swiss Federal Institute of Technology (ETH-Rat).

## References and Notes

- (1) Alexandridis, P.; Hatton, T. A. *Colloids Surf. A* **1995**, *96*, 1–46.
- (2) BASF Technical Brochure, BASF Co., Parsippany, NJ, 1989.
- (3) Tiberg, F.; Malmsten, M.; Linse, P.; Lindman, B. *Langmuir* **1991**, *7*, 2723–2730.
- (4) Malmsten, M.; Linse, P.; Cosgrove, T. *Macromolecules* **1992**, *25*, 2474–2481.
- (5) Freij-Larsson, C.; Nylander, T.; Jannasch, P.; Wesslén, B. *Biomaterials* **1996**, *17*, 2199–2207.
- (6) Green, R. J.; Tasker, S.; Davies, J.; Davies, M. C.; Roberts, C. J.; Tendler, S. J. B. *Langmuir* **1997**, *13*, 6510–6515.
- (7) Green, R. J.; Davies, M. C.; Roberts, C. J.; Tendler, S. J. B. *J. Biomed. Mater. Res.* **1998**, *42*, 165–171.
- (8) Brandani, P.; Stroeve, P. *Macromolecules* **2003**, *36*, 9492–9501.
- (9) Baker, J. A.; Berg, J. C. *Langmuir* **1988**, *4*, 1055–1061.
- (10) Shar, J. A.; Obey, T. M.; Cosgrove, T. *Colloids Surf. A* **1998**, *136*, 21–33.
- (11) Prestidge, C. A.; Barnes, T.; Simovic, S. *Adv. Colloid Interface Sci.* **2004**, *108–109*, 105–118.
- (12) Chen, C.; Even, M. A.; Chen, Z. *Macromolecules* **2003**, *36*, 4478–4484.
- (13) Elbert, D. L.; Hubbell, J. A. *Chem. Biol.* **1998**, *5*, 177–183.
- (14) Kenausis, G. L.; Vörös, J.; Elbert, D. L.; Huang, N.-P.; Hofer, R.; Ruiz-Taylor, L.; Textor, M.; Hubbell, J. A.; Spencer, N. D. *J. Phys. Chem. B* **2001**, *104*, 3298–3309.
- (15) Spencer, N. D.; Perry, S. S.; Lee, S.; Müller, M.; Pasche, S.; De Paul, S. M.; Textor, M.; Yan, X.; Lim, M. S. *Proc. 29th Leeds-Lyon Symp. Tribol.* **2003**, 411–416.
- (16) Lee, S.; Müller, M.; Ratoi-Salagean, M.; Vörös, J.; Pasche, S.; De Paul, S. M.; Spikes, H. A.; Textor, M.; Spencer, N. D. *Tribol. Lett.* **2003**, *15*, 231–239.
- (17) Müller, M.; Lee, S.; Spikes, H. A.; Spencer, N. D. *Tribol. Lett.* **2003**, *15*, 395–405.
- (18) Yan, X.; Perry, S. S.; Spencer, N. D.; Pasche, S.; De Paul, S. M.; Textor, M.; Lim, M. S. *Langmuir* **2004**, *20*, 423–428.
- (19) Ratoi-Salagean, M.; Spikes, H. A. *Tribol. Trans.* **1997**, *42*, 479–486.
- (20) Hamrock, B. J.; Dowson, D. *Proc. 5th Leeds-Lyon Symp. Tribol.* **1979**, 22–27.
- (21) Esfahanian, E.; Hamrock, B. J. *Tribol. Trans.* **1991**, *34*, 628–632.
- (22) Roberts, A. D.; Tabor, D. *Proc. R. Soc. London A* **1971**, *325*, 323–345.
- (23) Richards, S. C.; Roberts, A. D. *J. Phys. D* **1992**, *25*, A76–A80.
- (24) Moore, D. F. *Wear* **1975**, *35*, 159–170.
- (25) Medley, J. B.; Strong, A. B.; Pilliar, R. M.; Wong, E. W. *Wear* **1980**, *63*, 25–40.
- (26) Dowson, D.; Jin, Z. M. *J. Phys. D* **1992**, *25*, A116–A123.
- (27) Drews, M. J.; LaBerge, M. An investigation of the fatigue induced failure modes of fiber/elastomer composites as bearing surfaces in total hip joint prosthesis. In *National Textile Center Annual Report*; Nov 1996; pp 71–79.
- (28) Scherge, M.; Gorb, S. N. *Biological Micro- and Nanotribology*; Springer: Berlin, 2001.
- (29) Mansour, J. M. In *Applied Kinesiology*; Lippincott Williams and Wilkins: Philadelphia, PA, 2003; Chapter 5.
- (30) Hills, B. A. *Proc. Inst. Mech. Engrs. H* **2000**, *214*, 83–94.
- (31) Kurrat, R.; Textor, M.; Ramsden, J. J.; Böni, P.; Spencer, N. D. *Rev. Sci. Instrum.* **1997**, *68*, 2172–2176.
- (32) Vörös, J.; Graf, R.; Kenausis, G. L.; Bruinink, A.; Mayer, J.; Textor, M.; Wintermantel, E.; Spencer, N. D. *Biosens. Bioelectron.* **2000**, *15*, 423–429.
- (33) Höök, F.; Vörös, J.; Rodahl, M.; Kurrat, R.; Böni, P.; Ramsden, J. J.; Textor, M.; Spencer, N. D.; Tengvall, P.; Gold, J.; Kasemo, B. *Colloids Surf. B* **2002**, *24*, 155–170.
- (34) Vörös, J.; Ramsden, J. J.; Csúcs, G.; Szendro, I.; De Paul, S. M.; Textor, M.; Spencer, N. D. *Biomaterials* **2002**, *23*, 3699–3710.
- (35) Ramsden, J. J. *J. Stat. Phys.* **1993**, *73*, 835–877.
- (36) Tontisakis, A.; Hilfiker, R.; Chu, B. *J. Colloid Interface Sci.* **1990**, *135*, 427–434.
- (37) Lee, S.; Heuberger, M.; Rousset, P.; Spencer, N. D. *J. Food Sci.* **2002**, *67*, 2712–2717.
- (38) Chaudhury, M. K.; Whitesides, G. M. *Langmuir* **1991**, *7*, 1013–1025.
- (39) Smeeth, M.; Spikes, H. A.; Gunsel, S. *Tribol. Trans.* **1996**, *39*, 720–725.
- (40) Smeeth, M.; Spikes, H. A.; Gunsel, S. *Tribol. Trans.* **1996**, *39*, 726–734.
- (41) Tirrell, M. *Langmuir* **1996**, *12*, 4548–4551.
- (42) Choi, G. Y.; Kim, S.; Ulman, A. *Langmuir* **1997**, *13*, 6333–6338.
- (43) Rundlöf, M.; Karlsson, M.; Wågberg, L.; Poptoshev, E.; Rutland, M.; Claesson, P. J. *J. Colloid Interface Sci.* **2000**, *230*, 441–447.

MA049076W